Simulating millimeter-wave FMCW radar for standoff detection of body-worn explosives using full wave FDFD modeling

Justin L. Fernandes , Richard Obermeier, Carey M. Rappaport, and Jose A. Martinez
Work supported by Gordon - CENSSIS, BombDetec, ALERT, and Northeastern University, Boston, MA 02115 (justin.fernandes@gmail.com)

Abstract

The channel response of various targets is modelled and used to simulate different frequency modulated continuous wave (FMCW) radar configurations used for the detection of suicide bombers. The 2D finite difference frequency domain (FDFD) analysis is used to obtain the channel response of arbitrarily complex targets. The received signals of simulated FMCW waveforms are calculated and synthetic aperture radar (SAR) images are created using data from the full wave analysis. The waveforms and SAR images created show differences in threat and non-threat targets which may facilitate target identification.

Introduction

• The main objective is to simulate a *portable* radar system to detect *irregular contours* and materials on the surface of a human body [3].

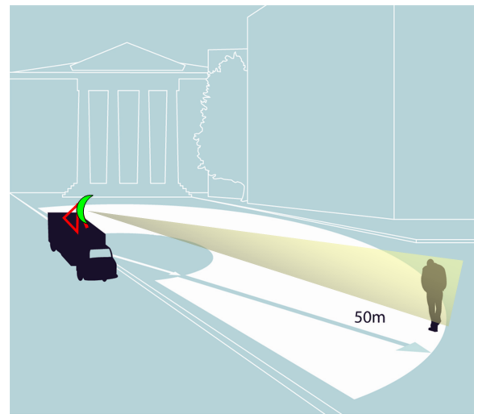

Figure 1: General sketch of a van-based, high resolution radar system for standoff detection of potential suicide bombers.

• Significant advantage to developing a wide-aperture multistatic radar. Multiple transmitters controlled simultaneously to illuminate small portion of the target chest, see Figure 2

• Inverse relationship between the size of the reflector and beamwidth of the radiation pattern. Use of higher frequencies ⇒ smaller reflector (more portable).

Model description

• In general there are three parts of a communication system.

Figure 2: Three parts of a communication system

• Transmitted signal of FMCW radar is:

$$s_t(t) = Re\{a(t)e^{j\Omega(t)}\}$$

• Channel impulse response is computed with FDFD analysis and near-field to near-field transformation:

$$G(\omega) = \Gamma(\omega)e^{j\phi_{\Gamma(\omega)}} = \mathfrak{F}^{-1}\{g(t)\}$$

• Received signal is the convolution of transmitted signal in time and channel time response:

$$h(t) = s_t(t) \bigotimes g(t) = \mathfrak{F}^{-1}\{G(\omega)S_t(\omega)\}$$

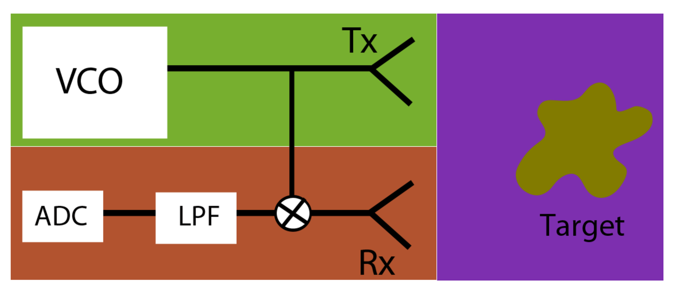

Figure 3: Diagram of basic FMCW communication system, Green = transmitter, Red = Receiver, Purple = Channel

• Transmitted signal of FMCW radar is:

$$s_t(t) = Re\{a(t)e^{j(\omega_o t + \pi\alpha t^2 + \phi_o)}\}$$

• Received signal is mixed with the transmitting signal producing an intermediate frequency signal:

$$s_{IF}(t) = Re\{s_t(t)\}Re\{h_t(t)\}$$

• Intermediate frequency is lowpass filtered, and range profile is obtained via the fourier transform:

$$\mathfrak{F}^{-1}\{s_{IF,LPF}(t)\} = S_{IF}(\omega)$$

Mutual Coupling

• Lack of full wave models which can compute radar cross section (RCS) of arbitrarily complex targets.

• 2D FDFD used to simulate a uniform plane wave incident on geometry in figure 4 A over 6 GHz bandwidth. Source and receivers are 1 meter "south" of scatterers (angle of incidence points north).

• Figure 4 D shows the result of mutual coupling between the two objects in figure 4 A.

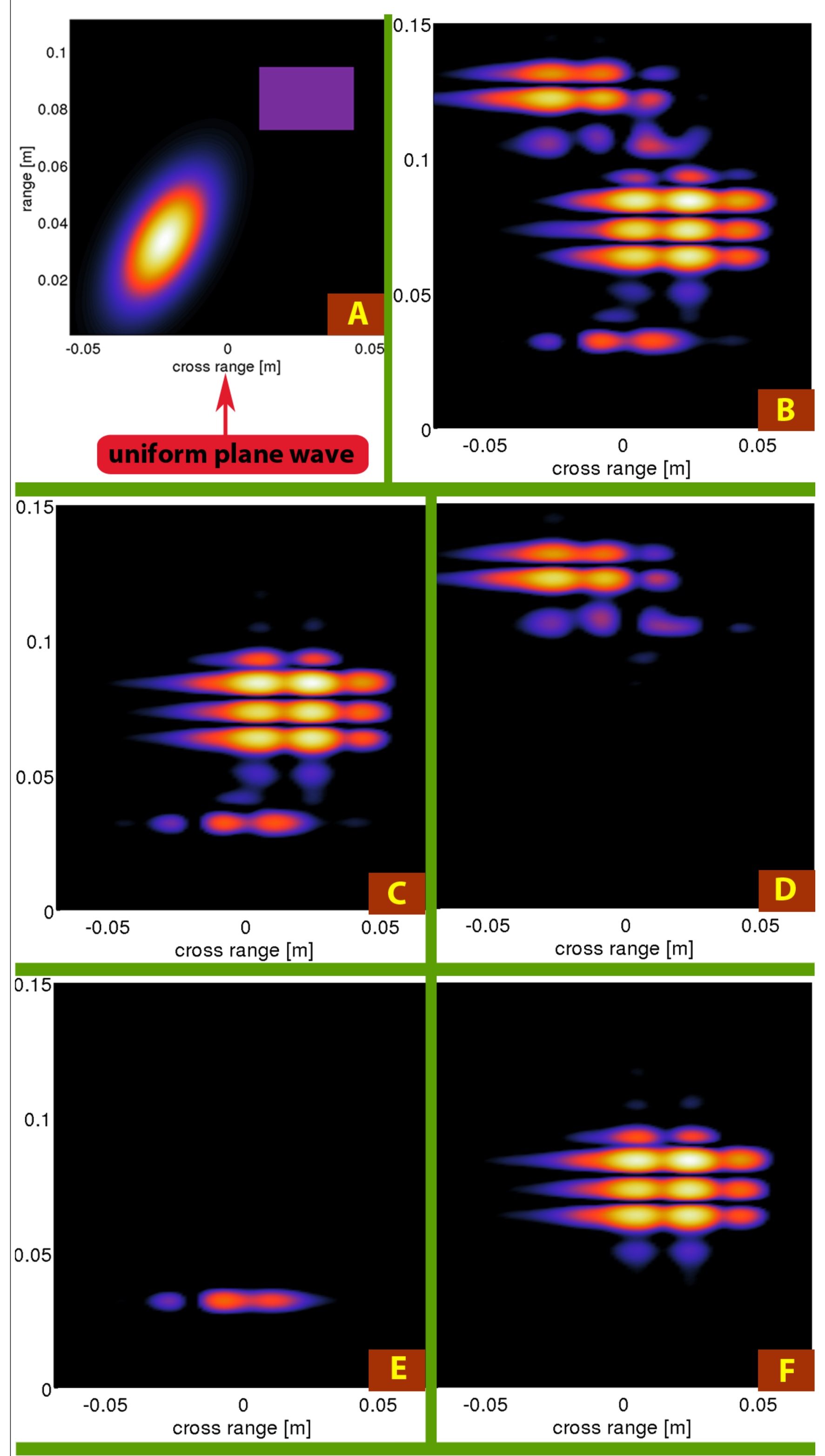

A. Geometry of scatterers used for FDFD simulation. Lower left is an elliptical dielectric shell with varying electric permittivity. Upper right is a square metal rectangle.

SAR reconstructed images using:

B. Full geometry field data.

C. Superposed field data of metal rectangle and dielectric layered ellipse (simulated separately).

D. Full geometry field data with superposed field data subtracted.

E. Dielectric layered ellipse field data.

F. Metal rectangle field data.

Figure 4: Mutual coupling analysis.

Results

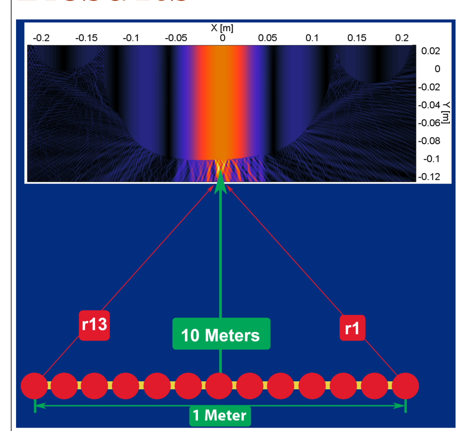

Figure 5: Simulation setup geometry. Each red circle denotes one of the 13 uniform plane wave sources on planar aperture.

Simulation Parameters:

• Bandwidth, $B = 8$GHz

• $N_f = 64$, number of frequencies over B

• $\Delta f = \frac{B}{N_f} = 125$MHz

• Uniform plane waves at 13 different incident angles per frequency.

• Range resolution $= \Delta R = \frac{c}{2B} = 0.01875$ [cm]

• Max unambiguous range: $R_{max} = \frac{c}{2\Delta f} = 1.2$ [m]

• Synthetic aperture size = 1 [m]

• Presence of pipes on target causes a large spread of power in SAR images due to more complex scattering, as was indicated in previous experimental data.

• Frequency response of threat target varies more sharply and is not periodic, as was indicated in previous experimental data.

Figures 6-9: • Top image is the geometry used for the FDFD analysis. • Middle image is the superposition of SAR image power as a function of incident transmitted angle, $\sum_{n=1}^{13} I(\theta_n)$ where $I(\theta_n)$ is the SAR image power. • Bottom image is the standard deviation of normalized pixel power as a function of incident transmitted angle.

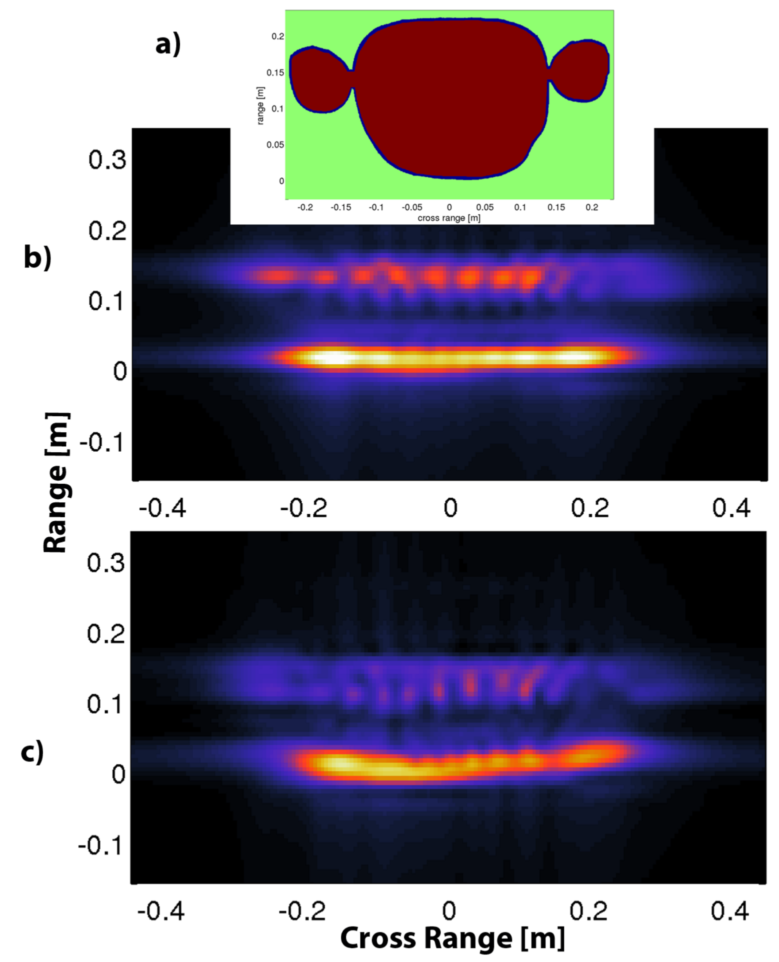

Figure 6: Male no pipes

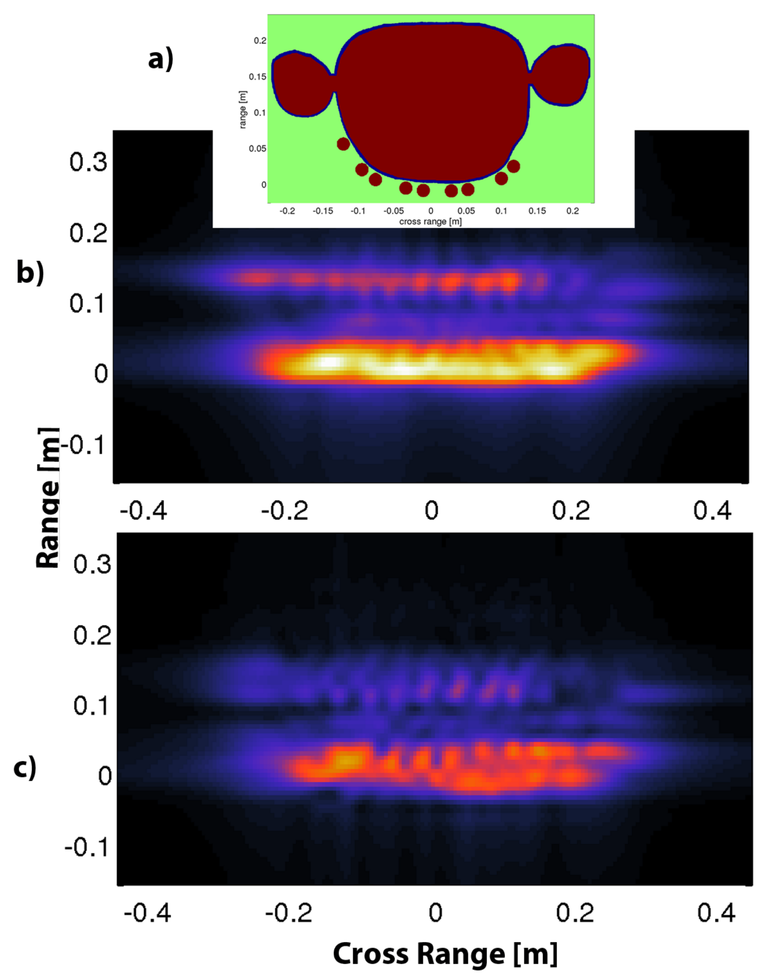

Figure 7: Male pipes

References

[1] P. Z. Peebles Jr., Radar Principles, New York: Wiley, 1998.

[2] Tessmann, e.t al., "Compact single-chip W-band FMCW Radar Modules for commercial high-resolution sensor applications," IEEE T. MTT, vol. 50. no. 12, Dec. 2002.

[3] Martinez-Lorenzo, J. A., Rappaport, C. M., et al. , "Standoff Concealed Explosives Detection Using Millimeter-Wave Radar to Sense Surface Shape Anomalies". , AP-S 2008, IEEE AP-S International Symposium, San Diego, CA, USA, Jun. 2008.

[4] Martinez-Lorenzo, J. A., Rappaport, C. M., Sullivan, R. and Pino, A. G., "A Bi-static Gregorian Confocal Dual Reflector Antenna for a Bomb Detection Radar System". , AP-S 2007, IEEE AP-S International Symposium, Honolulu, Hawai'i, USA, Jun. 2007.

[5] Sheen, D., McMakin, D., Hall, T., "Three-Dimensional Millimeter Wave Imaging for Concealed Weapon Detection," IEEE T-MTT, Sept., 2001.

[6] Rappaport, C., "High Resolution Thinned Array Synthesis Based on an Optimized Mapping Function," 1986 Antennas and Propagation Soc. URSI Symp. Digest, pp. 375-378, June, 1986.

[7] El-Shenawee, M., Rappaport, C., Miller, E., and Silevitch, M., "3-D Subsurface Analysis of Electromagnetic Scattering from Penetrable/PEC Objects Buried under Rough Surfaces: Application of the Steepest Descent Fast Multipole Multilevel (SDFMM)," IEEE T Geosci. Rem. Sens, 6/2001, pp. 1174-118.

[8] Rappaport, C., Dong, Q., Bishop, E., Morgenthaler, A., and Kilmer, M., "Finite Difference Frequency Domain (FDFD) Modeling of Two Dimensional TE Wave Propagation and Scattering," URSI Symp. Digest Pisa, Italy, May 16-18, 2004, pp. 1134-1136.

[9] John C. Curlander, Robert N. McDonough, Synthetic Aperture Radar: Systems & Signal Processing, John Wiley & Sons, Inc., USA, 1991.

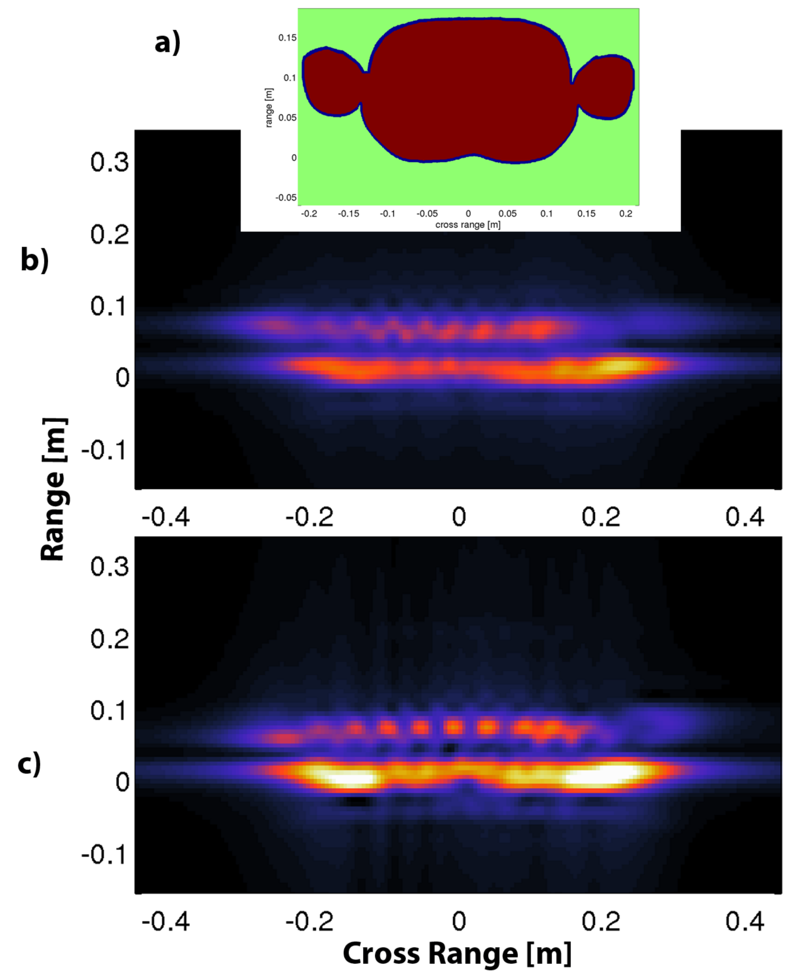

Figure 8: Female no pipes

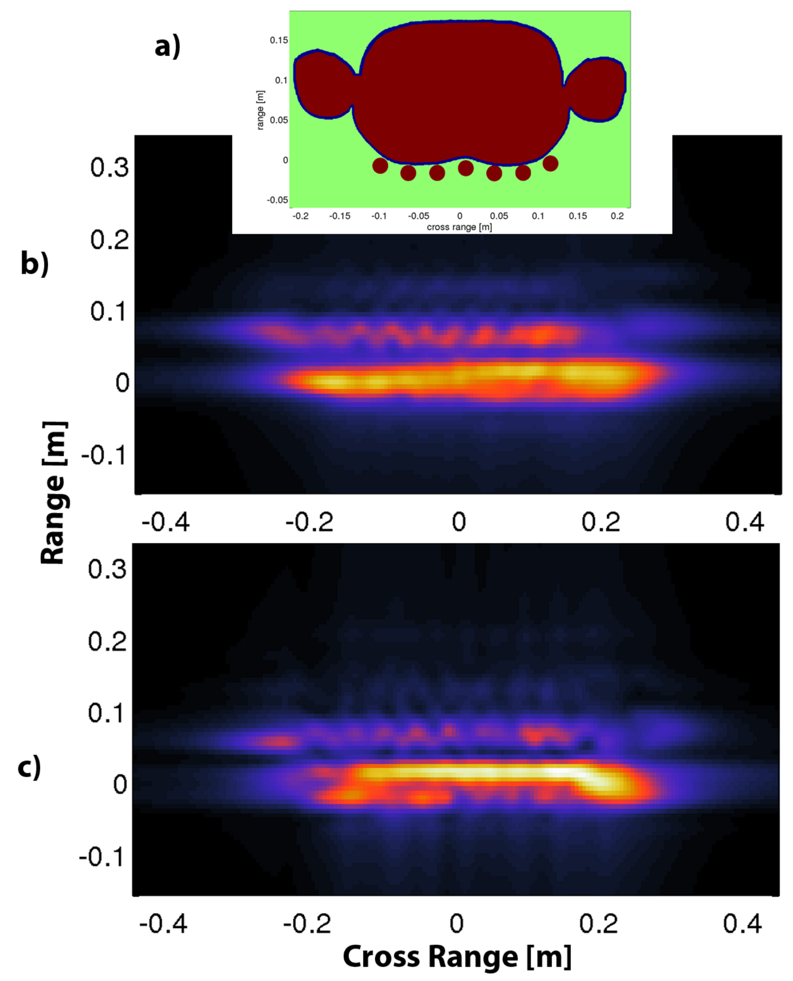

Figure 9: Female pipes

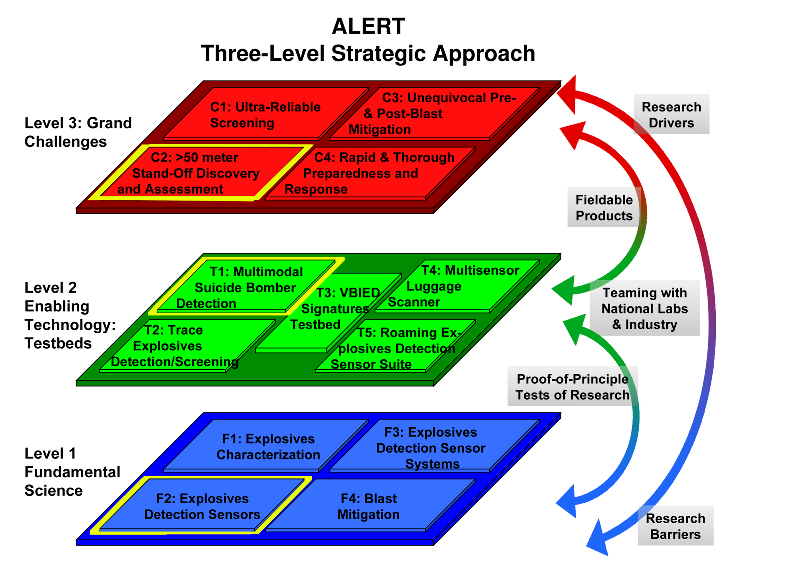

This material is based upon work supported by the U.S. Department of Homeland Security under Award Number 2008-ST-061-ED0001. The views and conclusions contained in this document are those of the authors and should not be interpreted as necessarily representing the official policies, either expressed or implied of the U.S. Department of Homeland Security.